# Using consumer drones in surveying deltas and coastal systems

**Student**: Nikolaas Sorgedrager

**Student number:** 3477088

**Masters and Institution:** Water Science and Management at University of Utrecht

**Supervisor:** Dr. Timothy Price (Faculty of Geosciences)

**Second Reader**: Prof. Jasper Griffioen (Faculty of Geosciences)

**Internship Company:** Shore Monitoring & Research

**Internship Supervisor:** Roeland de Zeeuw

Utrecht University

# Table of Contents

## Abstract

Due to rapid developments in the drone industry, low-cost high quality consumer drones are increasingly available to the general public. This research will explore the potential of drones in the field of delta and coastal surveying. Fieldwork was done in Myanmar and involved gathering topographic data to characterize the riverbanks of the Pan Hlaing River. One of the drone-based techniques used is photogrammetry to obtain a digital elevation model (DEM) and Orthomosaic. The other technique is rectification, a process whereby single images are transformed to a 2D map. The research focusses on the methodology of the two techniques, with special emphasis on the use of ground control points (GCP's), identifying factors determining accuracy and practical challenges in the field. GCP's derived from satellite imagery were successfully used, with as downside accuracy loss due to satellite map geo-referencing. The root-mean-square error (RMS) was used to identify accuracy. Average accuracy of the rectification end products was in the range of 10 – 40m. Camera lens distortion is identified as a major cause of accuracy loss. Future research should take in account lens distortion changes due to a changing focal distance. Photogrammetry was uncomplicated due to available software for both flying and processing, with the DEM having an accuracy of 1.5m. Further important factors identified to take in account for a successful drone survey are technical capabilities of the equipment used, law, regulation and ethical concerns.

# 1. Introduction

Deltas and coasts, being the interface between land and water, are one of the most dynamic and complex environments. Due to their richness in natural resources and unique geographic position, they are amongst the most densely populated areas worldwide. With an ongoing trend of further coastal migration and rising sea level due to climate change, deltas and coasts are increasingly under pressure. (Neumann et al, 2015).

With the majority of human settlements being close to or below sea-level, sea-level rise and storm activity due to a changing climate can have disastrous consequences in the form of flooding or erosion. On the other hand, man-made interventions can also have unintended consequences, changing the dynamics of the system and hereby accelerating erosion or decreasing water quality.

To adapt to the changes in deltaic and coastal systems, it is crucial to gain understanding of the state and dynamics of these systems. Obtaining data is the first step towards understanding the system, which can lead to formulating design criteria for adaptations and interventions (Webb et al., 2013). Gathering the data is done by surveying and monitoring. Surveying involves characterizing and mapping the system in its current state. Monitoring, being similar to surveying, involves multiple surveys over time in order to study changes within the dynamics of a system.

Within deltas and coasts, surveys on land and water have to be undertaken, often combining various techniques such as echo sounders and aerial imagery. From a technical perspective trade-offs are usually made between spatial coverage and accuracy. With plenty of established techniques to choose from, technical possibilities rarely form obstacles for surveying and monitoring. The main obstacle is usually a lack of resources in the form of money, time or skilled workers. Resource constraints are a reality for any organization interested in surveying and monitoring, ranging from Universities, NGOs to governments in 3rd world countries. Affordable and accessible technology would enable these organizations to conduct surveys and set up monitoring programs, allowing them to characterize and gain understanding of the system. This understanding is crucial to preserve the communities and ecosystems existing within delta and coastal areas.

Shore Monitoring and Research, the internship organization where this research is conducted, actively researches innovation of survey and monitoring methods. Developing a less resource intensive method would allow them to offer services to their clients at a fraction of the current cost, without the need to travel around with heavyweight expensive survey equipment. A promising new technique involves the use of lightweight UAV's (Unmanned Aerial Vehicles), more commonly known as consumer drones, which are relatively low-cost drones available to the public.

This thesis will focus on exploring the potential of consumer drones in coastal and delta surveying and monitoring, including a field study in Myanmar. Chapter 2 will give a brief overview of existing approaches along with relevant literature. Possibilities and drawbacks of using consumer drones will be explored, as well as synergies with other survey techniques. Together this will lead to the research questions of this paper. Chapter 3 will introduce the field site of research, together with a description of the main methods, photogrammetry and rectification, alongside with the materials used. Chapter 4 will consist of results following the field research. Both technical and practical challenges will be explored. In Chapter 5 the results will be discussed and evaluated. Chapter 6 will contain the conclusion, alongside with recommendations for future research.

# 2. The role of drones in Surveying and monitoring

## 2.1 Current state of drone based research

Consumer drones equipped with a camera, such as the Mavic Pro used for this research (Figure 1), have opened up new possibilities in the field of surveying. The development of consumer drones has taken a flight in recent years. Due to the relatively low purchase cost and the fact that little to no permits are needed to fly them, the number of consumer drones used by both hobbyists and professionals worldwide has dramatically increased.

Figure 1. [Mavic Pro in hand and in Flight]. (DrDrone.ca., 2018), (Goldman, 2016)

Due to the small size of consumer drones they are unable to carry a wide range of survey equipment such as LIDAR (Laser Imaging Detection and Ranging) scanners or high-end GPS (Global Positioning System) devices. This is also not the aim, as it would no longer classify as low cost. Instead the camera attached to the drone, included upon purchase, is used to obtain aerial imagery. There are numerous examples of the usage of drones in the scientific world, some of the applications and their perceived benefits compared to other techniques are discussed below.

(Bhardwaj et al., 2016) discusses the use of drones in the field of glaciology. Satellite remote sensing is an effective and traditional way to monitor glaciers and snowfields globally, however satellites are limited by spatial and temporal resolutions, as well as high costs involved with data acquisition. Compared to satellites, drones have advantages by being easy to deploy, having a high spatial resolution and allowing for data acquisition on your own schedule with minimal costs. An example of using the drone in glacier monitoring can be found in the work of (Immerzeel et al., 2014), who used a drone in concurrence with the technique of photogrammetry to construct a Digital Elevation Model (DEM) of a Himalayan glacier. By making two DEM’s at different points of time, the direction and velocity of glacier movement could be estimated (Figure 2).

Within a delta setting, (Hemmelder et al., 2018) used drone imagery for studying river morphology and dynamics. They used photogrammetry derived DEM’s for a quantitative assessment of bank erosion, whilst using OrthoMosaics, which is a 2D map made by connecting all undistorted photogrammetry images, for mapping the floodplains dynamics (Figure 3). The drones were said to be flexible and easy to use, noting that the imagery is processed in a straightforward way using modern software.

Some other examples are: (Chikhradze et al., 2015) using close range digital photogrammetry for monitoring and managing beaches in Portugal (Figure 4), (Guillot et al., 2018) using drones and photogrammetry techniques to monitor beach recovery from severe winter erosion in South-West France (Figure 4) and (Zhang et al., 2016) using a drone to make detailed maps of forest canopy structures (Figure 4). Most notable comments on the benefits of drones in these researches regarded the possibility to obtain low-cost data with a high spatial and temporal resolution together with flexibility and ease of use.

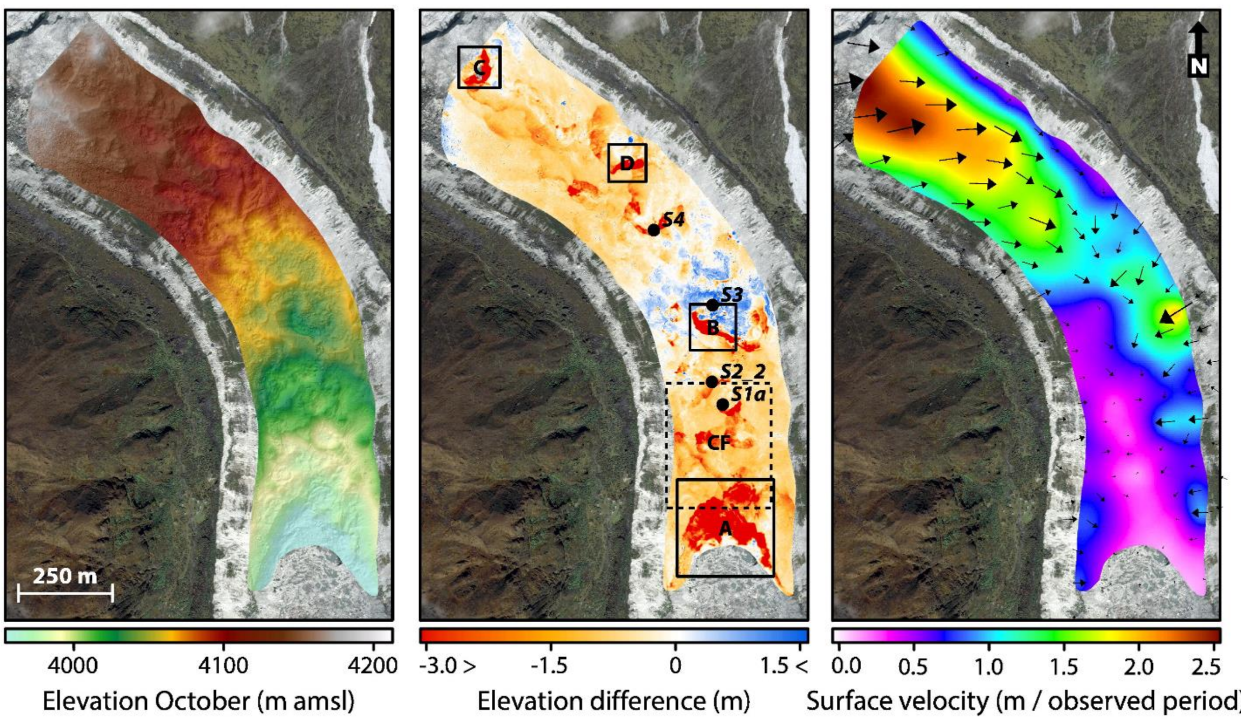


Figure 2. [DEM of a Himalayan glacier (left), Elevation difference between two DEM's (middle), Surface velocity of glacier based on the elevation difference over a given time period (right). (Immerzeel et al., 2014)

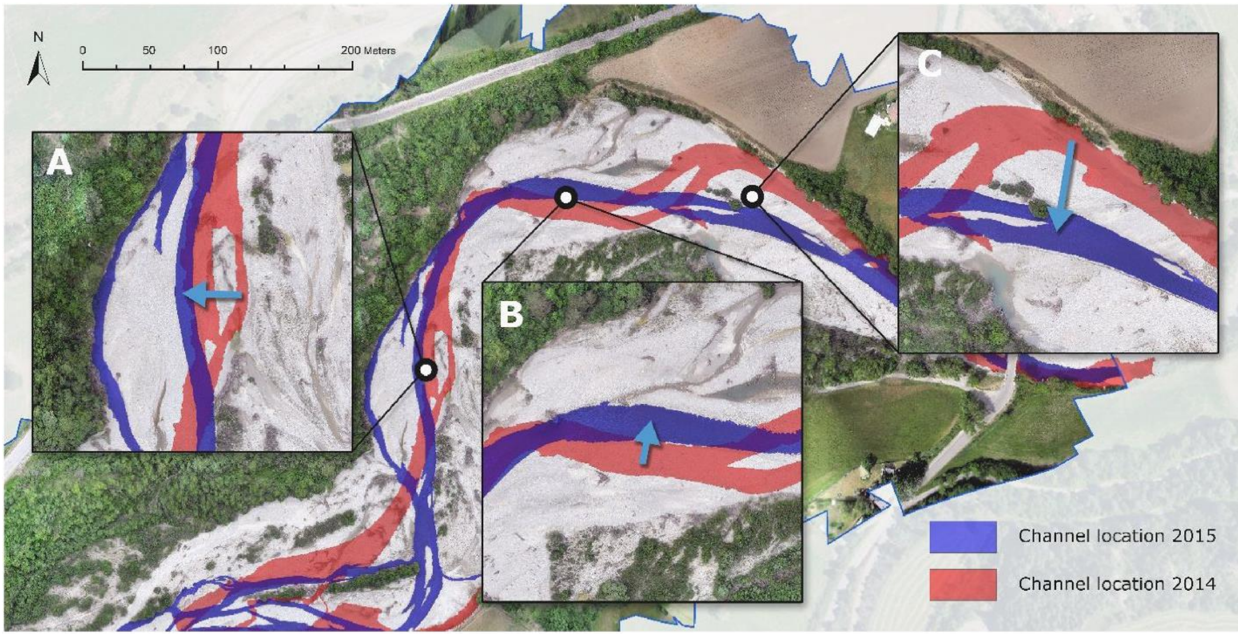


Figure 3. [Locations of the river channel in 2014 and 2015 derived from Orthomosaics and projected on an Orthomosaic, illustrating the movement of the channel from 2014 to 2015] (Hemmelder et al., 2018)

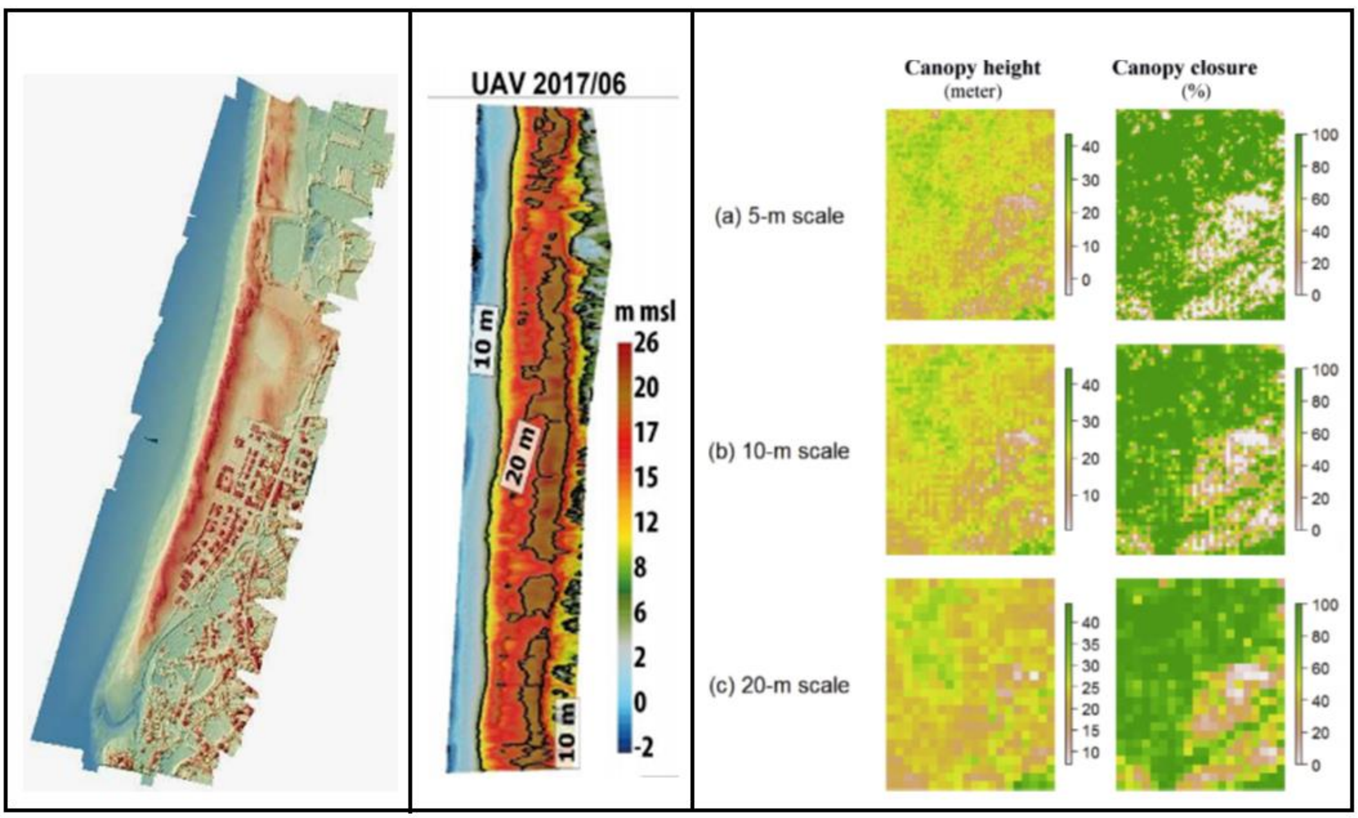


Figure 4. [(left) DEM of Aguçadoura beach in Portugal 2014 , (middle) Photogrammetry derived topographic map of Truc Vert beach SW France, (right) Canopy Height (m) and Canopy Closure (%) at

different scales, derived from drone based surveys.] (Chikhradze et al., 2015), (Guillot et al., 2018), (Zhang et al., 2016)

## 2.2 Research aim and questions.

Shore Monitoring & Research recently started exploring the possibilities of surveying and monitoring with drones. Their work includes the more established technique of photogrammetry, but also explores the use of image rectification. Rectification has been used traditionally in remote sensing by correcting for the slightly oblique angle found in aerial or satellite imagery (Wu, 1985), the main inspiration however was the use of rectification on the strongly oblique imagery captured by the ARGUS beach monitoring system ("ARGUS video systems - Deltares", 2018) (Figure 5). First experiments combining drones and rectification, conducted at SHORE by (Aarnink, 2017), have been promising.

Figure 5. [Example of Argus Video System setup for beach monitoring] ("ARGUS video systems - Deltares", 2018)

This research involves further developing a drone survey methodology for SHORE. Whilst the studies presented in section 2.1 mainly highlighted the benefits and possibilities of using drones, SHORE has indicated some drawbacks based upon their previous experience with drone surveys. Amongst them are the time and labor involved in finding or placing suitable Ground Control Points (GCP's), inherent distortion of camera lenses and the two-dimensional nature of rectification. The extraction of GCP's from satellite imagery has been suggested as one way of reducing GCP related labor intensity. Another point of interest is the combination of rectified material with vertical data from water-level loggers, which could broaden the possible applications of rectification and will be explored in this research. Other drawbacks and best practices are to be indicated and tackled whilst experimenting during a field project in Myanmar.

The structure of the research will be dictated by the distinction between photogrammetry and rectification techniques, which will be looked at from both a technical and a practical perspective. Based upon the results of the fieldwork, the factors dictating a successful drone survey will be discussed.

The resulting research questions are:

**Main research question:** *To what extent can consumer drones be used for surveying of deltaic and coastal systems?*

**Sub-question 1:** *Can fixed objects with coordinates derived from satellite maps serve as an alternative to manually placed ground control points?*

**Sub-question 2:** *Which are the main factors influencing the accuracy of the final products?*

**Sub-question 3:** *Which factors, not covered in the previous questions, should be taken in account for conducting a successful drone survey?*

# 3. Materials and Method

## 3.1 Field site

The field site is located around the Pan Hlaing River, situated in the Ayeryawady delta in Myanmar. The river is part of an estuary which ends in the Andaman Sea. The downstream end of the Pan Hlaing River connects to the Yangon River, near the town of Yangon. The upstream end connects to the Kokowa River and is closed off by the Mezali Sluice.

The Pan Hlaing River is of great importance as a source of irrigation water for the farmland situated on both shores, however it's usability for irrigation is under threat. Upstream inflow is variable caused by variations in the wet and dry season. The inflow of fresh water has decreased due to upstream water extraction. At the downstream side the Yangon River has been dredged, increasing tidal influence. Increased tidal influence causes more saline water to be pushed further in the Pan Hlaing River. The river, being rich in suspended sediment, suffers from sedimentation due to flocculation, caused by the interaction between fresh and saline water. Due to siltation, the river is unable to discharge enough storm water in the wet season, causing flooding which results in damage to croplands. Together with the inability to retain enough water in the dry season and increased salt water influence, the river becomes increasingly unfit for agricultural purposes. In order to ensure a reliable source of irrigation water for the future, it has been decided that intervention needs to be made to the Pan Hlaing River. Currently the availability of environmental data, on which a suitable intervention should be based, is scarce.

This research mainly focusses on the junction between the Pan Hlaing and Yangon River, which is also the proposed location of possible intervention. (Figure 6, Location 1) Located close to the coast, this area has the most tidal dynamics and is the pathway of saltwater infiltration. The riverbanks themselves are poorly accessible, as they consist out of a thick layer of mud, followed by dense vegetation when moving inland. The environment is challenging for non-aerial topographic measurements, and therefore considered a suitable location for testing the use drones. There will be additional rectification and photogrammetry campaigns in two other locations. One location is at a Cofferdam (Figure 6, Location 2) serving to retain freshwater in the Pan Hlaing River. The other location is near Mezali Village, where there is a sluice regulating fresh water inflow marking the upstream boundary of the Pan Hlaing river (Figure 6, Location 3). Quantifiable data of the latter two locations will not be covered in this research, however experience gained in working with GCP’s and gathering imagery that is deemed relevant to the research will be included.

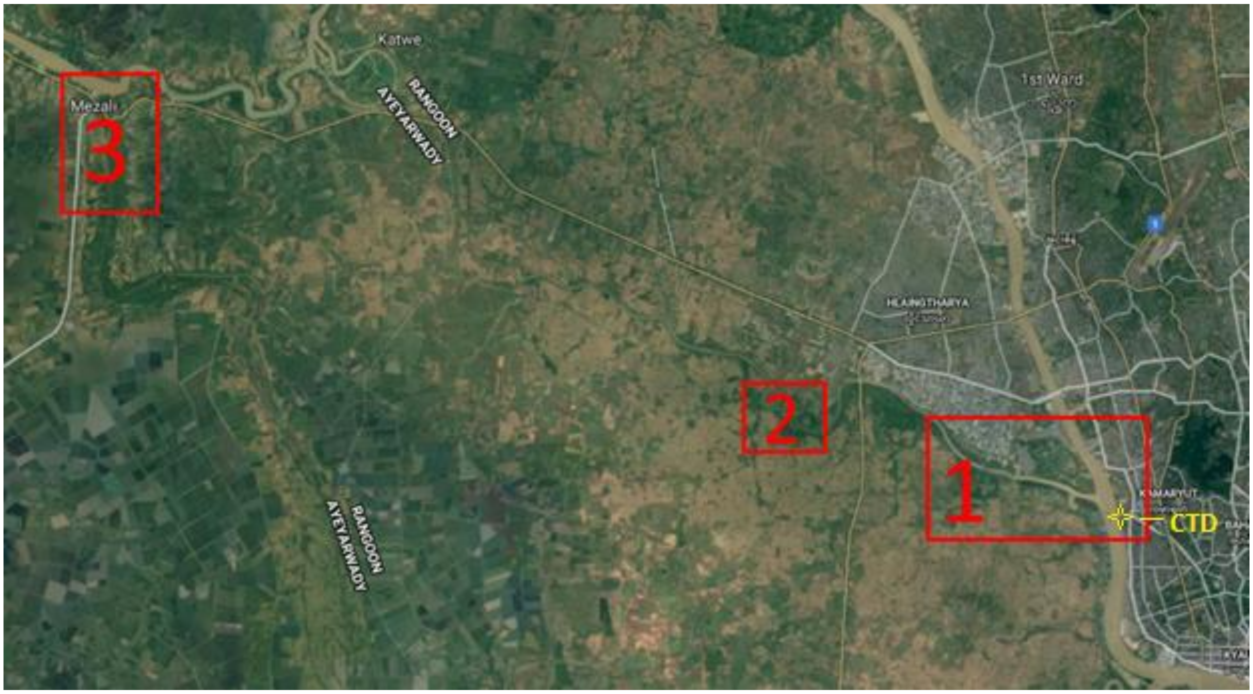


Figure 6. [Map containing 3 areas of research, 1: Pan Hlaing – Yangon River Junction, 2: Cofferdam, 3: Mezali Sluice. The water level logger used in this research is marked with yellow.] (Google Maps, 2018)

Figure 7. [View of Pan Hlaing River branching off the Yangon River]

Figure 8. [Cofferdam in the Pan Hlaing River]

Figure 9. [Mezali Sluice]

## 3.2 Field campaign

SHORE has been invited to survey the area to complement the currently scarce dataset of the area. The data will then become available to participants of a tender, to create a fair starting point as basis for an intervention plan to combat the issues in the Pan Hlaing River discussed above. The data will consist of bathymetry maps, discharge measurements, time series of water levels, salinity and temperature at various fixed points as well as salinity profiles along the Pan Hlaing and surrounding rivers. Of main interest for the drone research is the data gathered by the water level loggers. The loggers, also known as CTD (Conductivity, Temperature, Depth) sensors, were installed at both ends of the Pan Hlaing River to gain insight in the tidal dynamics and corresponding salt water infiltration. The loggers used are the CTD-divers produced by Schlumberger Water Services (Diver Manual, 2014) and were attached and referenced to fixed structures. The referencing was done by using RTK (Real Time Kinematic)-GPS, making use of a base station and rover.

The drone used for this research is a Mavic Pro quad copter, equipped with a 4k camera. Refer to the manual for further technical specifications of the Mavic Pro (Mavic Pro User Manual V2.0, 2017). Research done with the drone is considered experimental and will take place alongside the survey done by SHORE, but is not intended to be included in the dataset for the tender. Developing a drone methodology alongside a commercial field campaign allows for a realistic exploration of the challenges and possibilities of drone surveys, as well as offering the opportunity to explore synergies with other techniques in the field. The outcome of the drone based research will serve as an indicator of the applicability of the drone methodology in future field campaigns. The remainder of the method section will chronologically follow the steps of the drone methodology from data gathering to processing, visualization and analysis. Relevant techniques and materials used will be presented along the way. As indicated in the introduction, distinction will be made between steps relevant to the techniques of photogrammetry and rectification.

## 3.3 Gathering Imagery and Data

### 3.3.1 Ground Control Points

The first step before take-off is placing the GCP's and measuring the x,y,z coordinates of the GCP's. As stated by (Martínez-Carricondo et al., 2018), the most accurate DEM's and rectified images are obtained when the GCP's are evenly spread amongst the field, with a minimum requirement of covering all four corners of the research area. (Martínez-Carricondo et al., 2018) also recommend a sufficient density of GCP's, with an increasing density amongst objects of interest or places with a strong topographical variation.

There are multiple methods of creating GCP's, which can be manually placed objects (Figure 10), pre-existent man-made objects (Figure 10) or striking natural landmarks. Manually placed objects allow freedom of placement. Downsides involve the effort in making and placing them and their sensitivity to theft or displacement. Fixed manmade objects involve little effort other than measurement and perhaps highlighting them with paint. The downside is that man-made objects are not always available at the desired locations. Natural landmarks are similar to man-made objects in usage, an added downside is that they are often difficult to measure in rugged terrain such as the Pan Hlaing riverbanks.

Figure 10. [Two examples of self made GCPs (left), Pole of Electricity Mast used as GCP (right]

This research will make use of all three kinds of GCP's. The x,y,z coordinates will be measured with using RTK-GPS, having an accuracy in the millimeter range. As either placing or measuring GCP's in the field involves significant effort, this research will also explore the usage of satellite imagery for obtaining GCP's. Satellite imagery is already used in initial exploration of the research area, however x,y,z coordinates of both man-made objects and landmarks can also be obtained from satellite imagery, removing the need to measure GCP's in the field. The extent to which satellite imagery is usable for the purpose of obtaining GCP's will be explored in sections 4.1.1 and 5.1.3.

### 3.3.2 Water Level Loggers

Water level loggers are to be installed before take-off in order to have water level data at the time of image capture. A single water level logger was installed near the research area. The logger was attached to a bamboo pole, which was then attached to a fixed structure. The logger only records water level above the sensor, in order to obtain water level height in a coordinate system the location of the sensor has to be referenced. A benchmark, straight above the CTD, on the fixed structure was measured using RTK-GPS in a WGS84 coordinate system. To find the sensor location in WGS84, the vertical distance from the sensor to the reference point is recorded using measuring tape. Subtracting the vertical distance from the z-coordinate of the reference point will yield the x,y,z location of the logger.  The water level can then be expressed in WGS84 and used with the other data. Proper recording of the distances and coordinates involved will also allow for later checkups on movement of the sensor, which is crucial when the water level log shows unusual changes.

### 3.3.3 Flying and capturing imagery

*Photogrammetry*

A photogrammetry mission starts with identifying the area to be captured. Within the mission there is a choice between flight altitude and image overlap. A low flight altitude and high image overlap will yield the highest resolution, at the cost of time involved. Whilst a high flight altitude and low image overlap allows capture of a larger area in a shorter time span. A limiting factor is the lifespan of the batteries. This research involved the use of 4 Mavic smart flight batteries (Mavic Pro User Manual V2.0, 2017), together allowing an average flight time of 2 hours.

It is possible to fly the missions manually, but attaining consistent overlap and altitude is difficult. Free mission planning software, of the type PIX4D-planner was used in planning, auto-piloting and automatic image capture within the missions. An optimum was found between the highest resolution data of the desired research area, attainable within the lifespan of the batteries.

*Rectification*

A rectification missions starts with finding a location from which the research area is covered from a desired angle. A greater area can be covered by either taking images with a greater angle with respect to the ground or by increasing the flight altitude, increasing one or the other causes a decrease in overall resolution. The main limitation is flight altitude, which is 500m with respect to the takeoff point for the Mavic Pro, but which can be lower when adhering to local regulations.

The rectification mission was conducted using DJI GO (DJI Official, 2018), the flight software of the drone manufacturer. After the first flight a waypoint was set, so the next series of images could be made from roughly the same location. The camera was controlled manually.

## 3.4 Data processing

### 3.4.1 Camera Calibration

Lenses usually have significant distortion, which is a result of imperfections of the camera's internal geometry originating from the fabrication process. The distortion carries over to the captured imagery, resulting in inaccuracy. The two main types of distortions are radial distortion (Figure 11) and tangential distortion (Figure 12). Luckily this distortion can be accounted for, which starts with calibrating the camera to find the camera matrix of internal camera parameters and the matrix holding the distortion coefficients, a process of which the exact details are to be found in (Docs.opencv.org, 2018), an open source computer vision library usable within a python environment. The camera and distortion matrix will later on be used in the rectification process. Photogrammetry can make use of a predetermined camera matrix, but in this research the camera matrix will be generated by the photogrammetry software itself.

The cameras internal geometry and lens distortion was determined with a camera calibration script ("GoPro Lens Calibration and Distortion Removal", 2018) in Python. Although the script is aimed at go pro-lenses, the underlying principles remain the same and also apply to a wide angle lens, which is the lens type of the Mavic's camera. The distortion coefficients taken in account were three (k1 – k3) radial and two (p1 – p2) tangential distortion coefficients, assuming higher order coefficients do not cause significant distortion. The procedure involves taking at least 20 pictures of a checkerboard. The checkerboard should be photographed in different positions and under different angles, covering all corners of the camera lens, from both up close and from a distance. The number of squares, square crossing and the size of each square is known. Based on a comparison between the known size/shape of the checkerboard and the size/shape of the squares captured in the images, the camera intrinsic matrix and distortion coefficients can be calculated. Once the internal camera parameters and lens distortion are known, and assuming they don't change, they can be used indefinitely for that specific camera.

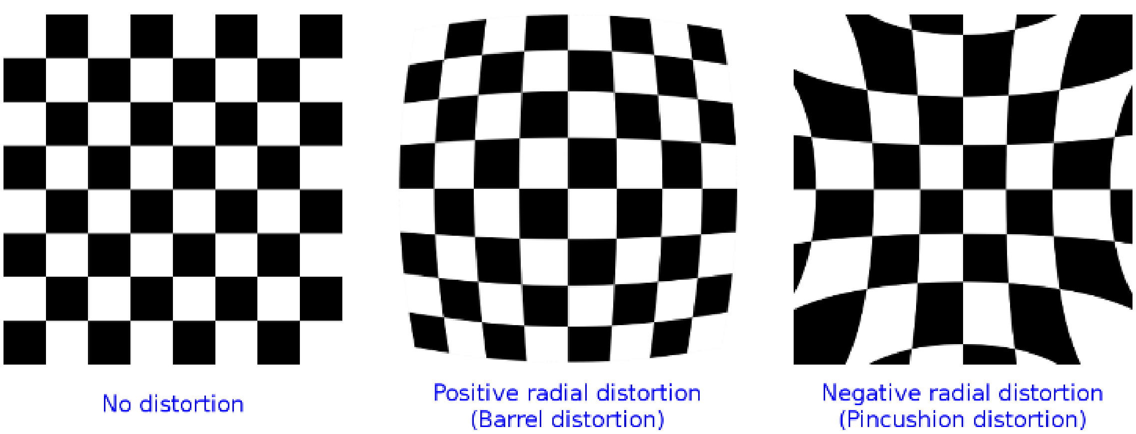


Figure 11. [Radial lens distortion] ("Camera Calibration and 3D Reconstruction — OpenCV 2.4.13.6 documentation", 2018)

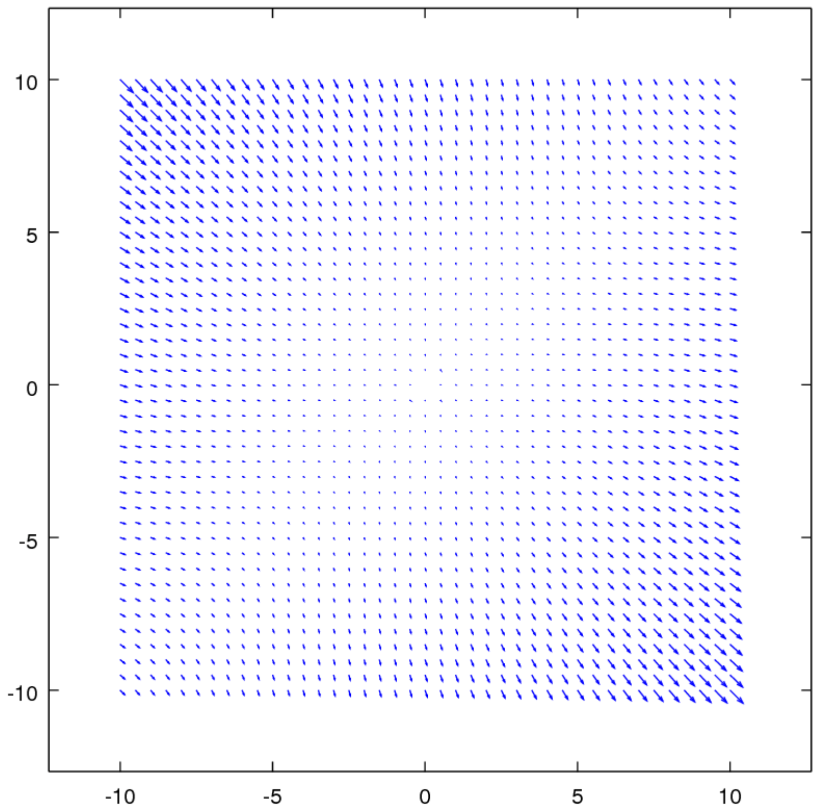


Figure 12. [Example of Tangential Distortion]

### 3.4.2 Rectification

When an image is taken with an angle other than 90˚ in relation to the ground and/or a fish-eye lens is used, the spatial coverage can be drastically increased, however it is not possible to do direct measurements of true distances within the image due to image perspective and distortion by the lens. Rectification is similar to rotating, stretching and shrinking the image and its individual U,V pixels to transform it into a 2D image representing true distances, referenced to a known x,y coordinate system. An example of 5 images from the Argus video system and their resulting transformations can be seen in (Figure 13).

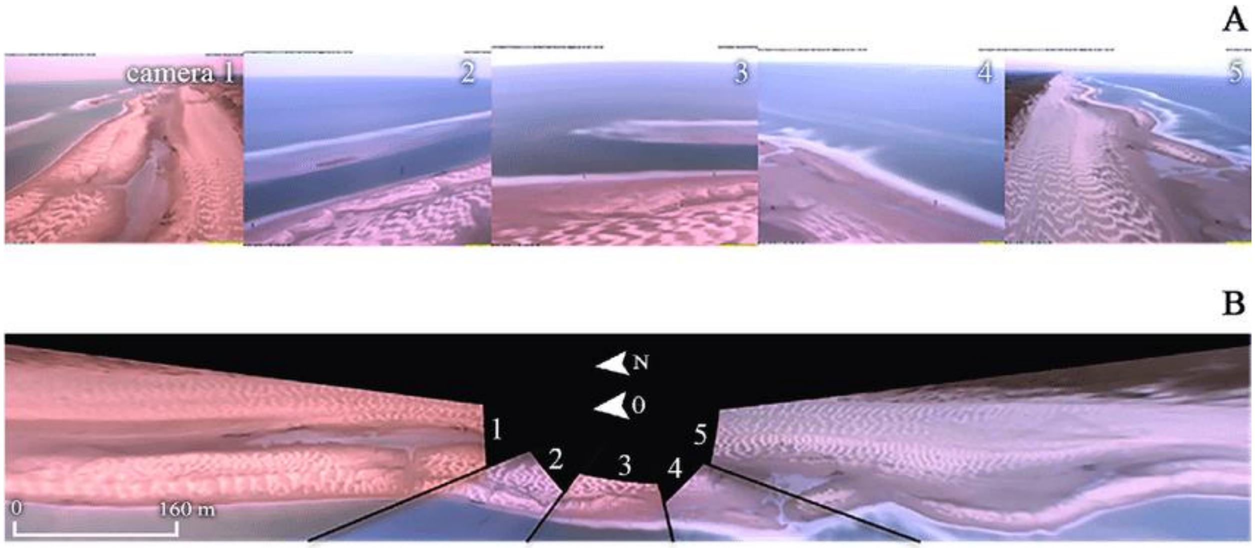


Figure 13. [Five Argus Images under different camera angles (top), The resulting 5 rectified images (bottom)] (Hage et al, 2018)

Rectification is done using Python, together with OpenCV (Opencv.org, 2018). The script used is a customized script based on the Flamingo Toolbox developed by (Hoonhout, 2014), which works with OpenCV. The key to rectifying an image involves the determination of its transformation matrix, also known as the homography. To find the homography a list of x,y coordinates containing the measured locations of each GCP is entered. Alongside this list another list of the corresponding U,V coordinates of each GCP is entered. The U,V coordinates are gathered manually and are retrieved by clicking on the respective GCPs in the untransformed image. Next the internal camera matrix and the distortion coefficient matrix are added. The calculation of the homography is thus based upon the corresponding U,V and x,y GCP list and the relative distances between these coordinates in both coordinate systems, as well as the distortion found by calibrating the camera. The homography is the best fit found for transforming each individual coordinate to the new X,Y system.

After rectification the result is a X,Y coordinate matrix, holding transformed locations for each U,V coordinate. The U,V coordinates have individual colors represented in a RGB (red green blue) value matrix. The transformed image is made by making a mesh out of the X,Y coordinates and the RGB values tied to the corresponding the U,V coordinates. The mesh can then be plotted on the x and y axis of the coordinate system, creating the rectified image.

### 3.4.3 Rectified imagery, Water level Data and GIS

The rectified image can be further analyzed and edited in a Geographical Information System (GIS). In this research the software package ArcGIS is used. By plotting the mesh on predetermined axis, the coordinates of each corner of the image are known. The GDAL (Geospatial Data Abstraction Library) application within ArcGIS allows for saving the corner coordinates within the images metadata, which is the process of geo-referencing the image. Afterwards the image can be projected in ArcGIS at the right location in the desired coordinate system. Having a geo-referenced image opens up new possibilities, such as a visual comparison of the image location projected on a map application such as Google Maps or allowing to make absolute measurements of distances and objects within the image.

Measurements done in ArcGIS were used together with the water level data to construct a contour map of the riverbanks. Water level data is available at an interval of 15 minutes, thus a water level at the moment of image capture can be derived. Knowing the water level is the same as having z-coordinates at any point along the waterline. The waterline can be tracked in ArcGIS, which will be stored in a shape file containing the x,y coordinates of the waterline. The z-value is then assigned to it, which will result in a x,y,z contour line at the interface of the waterline and the riverbank. This process will be repeated in images from low tide throughout high tide, resulting in riverbank contour line of the intertidal zone.

### 3.4.4 Photogrammetry

Although photogrammetry is a broad field of study with no consensus on a universally accepted definition, the definition: “Photogrammetry is the science of obtaining reliable information about the properties of surfaces and objects without physical contact with the objects, and of measuring and interpreting this information.” offered by (Schenk, 2005) captures the most important notion of photogrammetry.

Within the field of photogrammetry, this research focusses on obtaining geometric information resulting in a DEM trough the technique of aerial triangulation (Schenk, 2005). The processing software used for generating DEM’s is Agisoft Photostudio. An in depth explanation of the photogrammetric process is not within the scope of this research, but the basic photogrammetric workflow when using Agisoft Photostudio will be outlined below:

1. The photos are aligned, aided by the coordinates of image capture saved in the metadata of each image. The software tries to recognize and tie as many points as possible within overlapping images, resulting in a mosaic of images.
2. The list containing x,y,z coordinates of the GCP’s, are loaded in photo scan. The software will initially place the GCP’s on their approximate location within the mosaic. After initial placement there is a need for manual fine-tuning, by dragging the GCP’s to the exact GCP location on each image where they are found.
3. When all the GCP’s are placed, a low quality 3D point cloud is generated. Within the point cloud extreme outliers should be manually erased. The outliers are often the result of vegetation or water, which is poorly handled by the software. After manual fine tuning a high quality 3D point cloud is generated.
4. The high quality point cloud can be used to generate the desired final product in the form of a DEM and an OrthoMosaic.

## 3.5 Data Accuracy Analysis

A quantitative accuracy analysis of the rectified images is made using both GCP’s and checkpoints (CP’s). Checkpoints, just like GCP’s are points with a known position, however CP’s are not used in determining the homography. The CP’s are unused GCP’s derived both from GPS measurements or satellite imagery. The accuracy analysis will look at the location shift of each GCP and CP from their initial position to their position after rectification. The location shift is expressed in an X and Y component or residual, from the residuals follows the

Root-Mean-Square (RMS) error, the method of which is expressed in (Formula 1) and visualized in (Figure 14).

$$R_i = \sqrt{XR_i^2 + YR_i^2}$$

**$R_i$ = The RMS error of $GCP_i$**

**$XR_i$ = The X residual of $GCP_i$**

**$YR_i$ = The Y residual of $GCP_i$**

Formula 1. [Calculation of the RMS error of an Individual GCP]

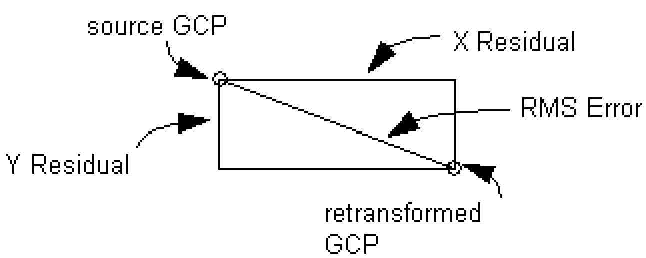


Fig 14. [Transformation of a GCP location and its components for calculating the RMS error]

The residuals of each individual GCP can be used to calculate the total RMS error (Formula 2).

$$R_x = \sqrt{\frac{1}{n}\sum_{i=1}^{n} XR_i^2}$$

$$R_y = \sqrt{\frac{1}{n}\sum_{i=1}^{n} YR_i^2}$$

$$T = \sqrt{R_x^2 + R_y^2} = \sqrt{\frac{1}{n}\sum_{i=1}^{n} XR_i^2 + YR_i^2}$$

**$R_x$ = the total X-RMS**

**$R_y$ = the total Y-RMS**

**T = The total RMS**

Formula 2. [Calculation of the combined RMS error]

The RMS error can also be expressed in pixel shifts instead of meters. For this the inverse of the homography is taken, which can be used to calculate the new location of each GCP expressed in transformed U',V' pixel coordinates. When knowing the old and new pixel locations, the remainder of the RMS calculation stays the same, with the only difference being the substitution of X, Y residuals by U, V residuals.

The accuracy of photogrammetry is expressed as an RMS in meters. The calculations are similar and done automatically by Agisoft, resulting in a list of individual GCP RMS values and a total RMS.

# 4. Results

The result section will be based on the chronology of the Materials and Method section, however it should be noted that the actual research process did not entirely follow the chronology of the methodology. Due to the explorative nature of the research there have been jumps between and revisions of various methodological steps. Yet the results will be presented, where possible, within the methodological framework in order to present the results in a coherent way. Qualitative results gained through experience in the field, not directly related to technical challenges of the methodology, will also be included.

## 4.1 Gathering Imagery and Data

### 4.1.1 Ground control points

At the Pan Hlaing – Yangon river junction (Figure 6) a total of 7 GCP's, consisting of fixed objects and landmarks, were recorded with GPS. The GCP's were recorded in the WGS84 coordinate system, having an accuracy in the millimeter range, with a maximum range of 20mm. Another 7 GCP's have been measured using Google maps. It was not possible to determine the exact accuracy of these points, as there was no reference value available. The overall accuracy of the geo-referencing of Google Maps within the research area was approximated by comparison of all the GPS measured points to their corresponding locations in Google Maps, yielding in an average accuracy difference of 3.72m. The locations can be found in (Figure 15)


Figure 15. [GPS GCP's shown in green, Google Maps GCP's shown in orange. The Drones approximate location for Rectification image capture is marked with yellow] (Google Maps, 2018)

Manually placed GCP's were not used in the Pan Hlaing – Yangon River fieldwork area, due to the high population density making movement of GCP's highly likely. The resulting usage of fixed objects and landmarks as GCP's also posed difficulty due to the limited availability of these objects and landmarks. Some objects and landmarks could not be accessed due to rugged or private terrain.

Manually placed GCP's were used in the two nearby locations of the Cofferdam and Mezali Sluice. The areas were both sparsely populated with small villages nearby. At the Cofferdam one GCP was removed, later to be found in nearby bushes, whilst at Mezali Sluice multiple GCP's were removed, not to be found again.

### 4.1.2 Water Level Loggers

The water level logger was fixed to a concrete jetty in the Yangon River, close to the point where it branches of into the Pan Hlaing River, its geographic location is indicated in (Figure 6). The water level time series are visualized in (Graph 1).

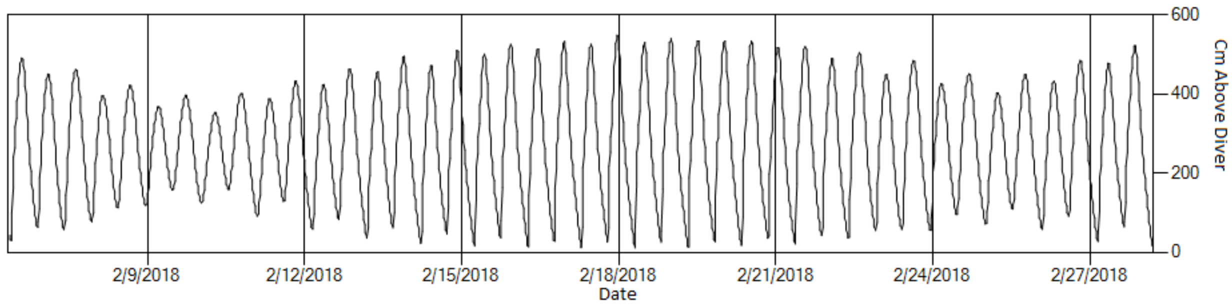


(Graph 1) Water level record of the Yangon River. Height is given in (cm) above the diver.

The graph shows the water level above the diver, for further use the water level data was transformed to the WGS84 coordinate system, following the steps described in the methodology.

Finding for a suitable location of the water level logger had been difficult. The main prerequisite for installing the logger was the availability of a fixed structure to attach it to, which should for part be permanently underwater. Preferably the water level logger was installed in the Pan Hlaing River closer to the research area, but the lack of such a fixed object resulted in the installing of the logger in the Yangon river as close as possible to the Pan Hlaing River.

### 4.1.3 Flying and capturing imagery

Rectification missions were done in a period ranging from low tide to high tide. During this period there where 5 moments of image capture, the approximate location of image capture is shown in (Figure 15). The moments were chosen upon visual inspection of significant tidal changes. The altitude of image capture was ~200m. Out of the batch of images, 5 images were chosen, each representing a distinct stage of the tide. (Figure 16) shows one of these 5 images at the lowest stage of the tide, including markers indicating the location of the GCP’s. This image is used as a base image for optimizing rectification, the remaining 4 images will be presented and rectified towards the end of the rectification process.


Figure 16. [Locations of the GPS (green) and Google Maps (orange) GCP's on picture to be rectified]

The photogrammetry missions were done during low tide, in a period of little tidal movement. The missions were flown at an altitude of 70m, referenced to the take-off zone. The overlap of images was set to 80%. A total of four missions, together roughly taking 2 hours were used to cover the selected research area, resulting in 1207 images covering an area of 0.599km$^2$. Preferably a bigger area was covered, however with no recharge option in the field, battery time was limited. An example image, taken near the location of GCP 1, as well as the approximated area covered is shown in (Figure 17).


Figure 17. [The yellow raster indicates the approximate area cover with photogrammetry (left), Example image of the Photogrammetry mission (right)]

The preparation before the flying has not been uneventful. The fieldwork was conducted in collaboration with the Ministry of Agriculture and Irrigation. Upon presenting the plan to use a drone, they raised concerns about law and regulation, especially for flying at the Pan Hlaing – Yangon river junction. Whilst there were no clear regulations for usage of drones, the advice was to keep the drone on the ground until permission was given by the mayor of Yangon. Two weeks later, after presenting a flight plan stating the details of when and how the flights would be conducted, permission was granted. Other than a loss of time, it caused difficulty with the availability of the GPS apparatus, which resulted in having to select and measure GCP's in the two weeks prior to take-off. A view from above would have helped to indicate the best places to select GCP's.

Flying itself has also not been uneventful. On one occasion hostility has been encountered, in the form of multiple angry locals, during the flying of the drone. A local taxi driver de-escalated the situation and explained us that the citizens were afraid that we were working for the government, as they had a dispute with the government on illegal housing in the area. Other times the work has been difficult due to being accompanied by hordes of curious children.

## 4.2 Data Processing

### 4.2.1 Camera Calibration

A total of 68 images were used for calibrating the camera. An example image can be found in (Figure 18.)

Figure 18. [One of the 68 images used for camera calibration]

The calibration was done inside an office. The images were taken under different angles and at different distances, ranging from approximately 0.5 to 5 meters from the checkerboard.

The resulting internal camera matrix is:

| | | |
|---|---|---|
| 2.33E+03 | 0.00E+00 | 1.97E+03 |
| 0.00E+00 | 2.34E+03 | 1.45E+03 |
| 0.00E+00 | 0.00E+00 | 1.00E+00 |

The resulting distortion coefficients are:

| | | | | |
|---|---|---|---|---|
| 3.50E-03 | -1.86E-02 | -1.25E-03 | 9.11E-05 | 1.14E-02 |

The reprojection error calculated after the calibration was:

| |
|---|
| 0.046456 pixels |

### 4.2.2 Rectification

Rectification has been an extensive process involving trial and error to explore the contribution of various variables and parameters on the results. In total there are 4 steps in the rectification process. The first step aims at finding the optimal setup using only GPS based GCP's, the second step also includes satellite derived GCP's, the third step involves exploration of the role of the camera parameters and the final step concludes with rectification of all 5 selected images, using the optimal setup of GCP's and camera parameters as found in the previous steps.

The consecutive steps were guided by quantitative improvements based on RMS calculations, as well as visual comparison in QGIS of geo-referenced rectified images against Google base maps. All GCP's, both from Google maps and from GPS, were used in the total RMS calculation, with the GCP's not used for rectification being labelled as checkpoints. The optimal setup of variables and parameters was defined as the setup yielding the lowest RMS. When selecting an optimal setup there was also attention to the replicability. When trying to replicate a result the total RMS was often similar but exact replication has not been achieved, whilst some attempts at replication lead to significant differences in total RMS. Therefore an optimal setup was only chosen if the total RMS is lowest compared to other results and the total RMS could be replicated with a deviation of maximum 10% from the initial result. The remainder of this section will discuss each individual step and the choice of GCP's used, an overview of the GCP's used in each of the 4 steps can be found in table 1.

| **GCP's** | **Step 1** | **Step 2** | **Step 3** | **Step 4** | **Notes Step 4** |
|---|---|---|---|---|---|
| GPS 1 | x | x | x | x | |
| GPS 2 | | | | | |
| GPS 3 | x | x | x | x | |
| GPS 4 | x | x | x | x | |
| GPS 5 | x | x | x | x | Not used in image 5 |
| GPS 6 | x | x | x | x | Not used in image 4, 5 |
| GPS 7 | | | | | |
| GPS 8 | | | | | |
| GMAPS 1 | | | | | |
| GMAPS 2 | | x | x | x | |
| GMAPS 3 | | | | | |
| GMAPS 4 | | x | x | x | |
| GMAPS 5 | | | | | |
| GMAPS 6 | | | | | |

Table 1. An overview of the GPS and Google Maps based (GMAPS) GCP's used in each rectification step.

**Step 1:** The first step involved finding the optimal setup of GCP's to use, whilst only using GPS measured GCP's for rectification. Including GCP 8 in the set of GCP's influenced the total RMS in such a manner that it overshadowed the contribution of the other GCP's, also replication was especially difficult when using this GCP. Inclusion of GCP 2 and 7 lead to a lower RMS for some of the neighboring GCP's and CP's, however inclusion of these GCP's consistently led to a higher total RMS.

The optimal setup thus included using GPS GCP's [1,3,4,5,6] (Fig 19). The lowest total RMS found in this case was: **77.65 m**.


Figure 19. [GCP's used for first step of rectification marked yellow, unused GCP's are marked red].

A visual inspection of the rectified imagery, as well as inspection of the RMS values warranted further optimization. Relatively large RMS values were found for the CP's in the upper 2/3 of the image.

**Step 2:** The second step includes usage of 6 GCP's based upon Google Maps. The Google Maps based GCP's have been selected with the intention to cover the parts of the image that are not covered by the GPS based GCP's. The final setup of GPS based GCP's from step one has been carried over to this step and left unchanged. Inclusion of Google Maps GCP's [1, 5, 6] significantly heightened the total RMS, whilst also causing difficulties of replication. Including Google Maps GCP [3] slightly elevated the total RMS. After trial and error using multiple combinations of Google Maps based GCP's, the optimal setup found included using Google Maps GCP's [2,4] together with the GPS GCP setup [1,3,4,5,6] from step 1 (Figure 20). The total RMS found in this case is **48.96 m**


Figure 20. [GCP's used in step 2 marked yellow, unused GCP's are marked red]

Visual inspection and inspection of the RMS still warranted further optimization. Notable was that the residuals found consistently were in the positive X and negative Y direction for each individual GCP.

**Step 3:** No further optimization could be found by adjusting the GCP's used, therefore the third step involved going back to the foundation and exploring the influence of the camera calibration. An additional camera matrix and list of distortion coefficients were obtained from photogrammetric work. Whilst it is possible to start photogrammetric work with a pre-determined camera calibration, based upon experience by SHORE photogrammetry yields the best results by not starting off with a predetermined camera calibration. Instead a camera matrix and distortion coefficients are calculated based upon the transformative calculations done during construction of the final photogrammetric model.

To test the effect of the camera calibration on rectification the GCP setup of step 2 was used. New homographies were calculated using combinations of different camera parameters. These new combinations involved making combinations using the original camera matrix, Agisoft camera matrix, original distortion coefficients and Agisoft distortion coefficients. Further tests involved manually changing the individual components of both the camera matrix and the distortion coefficients to study their individual contribution to the rectification accuracy.

Usage of the Agisoft camera parameters lowered the total RMS. Further exploration of the individual components revealed that disregarding the distortion yielded the lowest RMS values, with the elimination of tangential component having the greatest contribution of lowering the total RMS. (Table 2) contains a selection of total RMS values using various combinations of parameters, with usage of the Agisoft camera matrix and disregarding the distortion causing the lowest total RMS.

| Camera Matrix Tests and resulting total RMS (m) | |
|---|---|
| **Setup (Camera Matrix, Distortion Coefficients)** | **Total RMS (m)** |
| Original K and Distortion | **48.96** |
| Original K, Agisoft Distortion | **25.01** |
| Original K, No Distortion | **28.48** |
| Agisoft K and Distortion | **18.10** |
| Agisoft K , No Distortion | **10.35** |

Table 2. [Total RMS for Rectification carried out with varying camera parameters with K being the camera internal parameters]

**Step 4:** With the optimal GCP setup from step 2 and the camera parameter setup from step 3, all five images have been rectified (Figure 21). In this final step, additional to the total RMS in meters, the RMS expressed in pixel values has also been calculated. The meter and pixel RMS for each individual image can be found in (Table 3). It should be noted that for image 4 Google Maps GCP 6 was not used and for image 5 Google Maps GCP's 5 and 6 were not used, due to a slight variation in camera angle they were not recorded on the image.

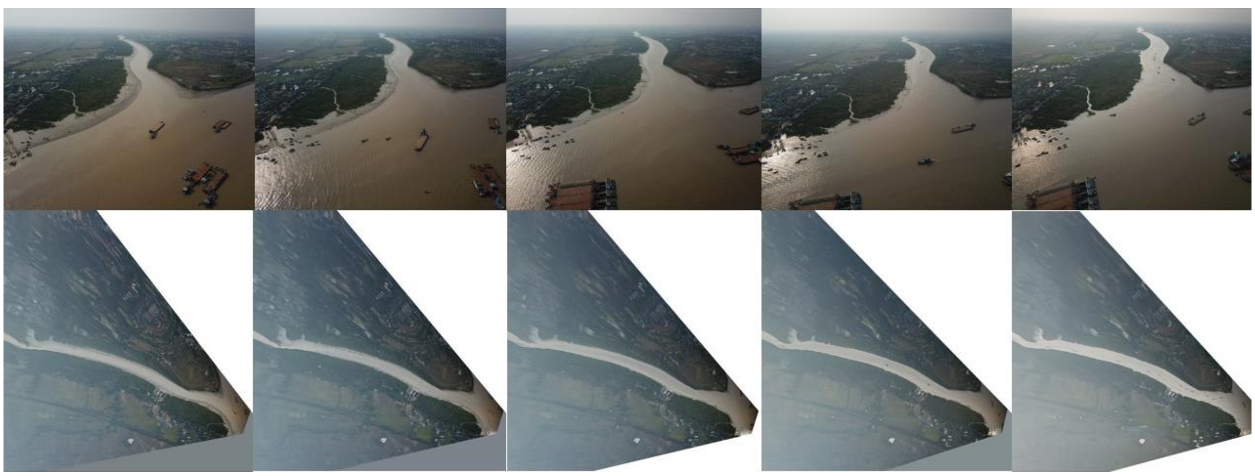

Figure 21. [All five images with their rectified counterpart below]

| Image Nr. | Total RMS meters | Total RMS pixels |
|---|---|---|
| **1** | 14.68 | 12.83 |
| **2** | 12.47 | 12.83 |
| **3** | 24.09 | 10.10 |
| **4** | 16.72 | 11.35 |
| **5** | 39.89 | 13.95 |

Table 3. [Total RMS in Meters and Pixels of all 5 Images]

### 4.2.3 Rectified Imagery, Water Level Data and GIS

The water level data was used to add a three dimensional component to the two dimensional rectified images. In each of the 5 images, the water line was manually tracked in QGis, resulting in an x,y vector line for each waterline. The moment of image capture for each image is known and the corresponding water levels were retrieved from the water level data. The water level values were added to the tracked waterlines. The result is five lines which are contour lines of the riverbanks holding x,y,z values. (Figure 22) shows a zoomed out perspective of the contour lines, whilst (Figure 23) offers a closer inspection on the contour lines. The height values are currently expressed as the height of the water column above the sensor of the water level logger. Since the water level loggers have been referenced to the WGS84 coordinate system, the values can also be expressed in WGS84 and from that point on converted to any coordinate system that is related to WGS84. The last part of the image, not captured in (Figure 22), contains no contour lines. The resolution in that part of the image was too coarse to distinguish the border between the water and the riverbanks.

Figure 22. [Rectified image, projected on a satellite background map (Digital Globe, 2018), including waterline contours for 5 stages of the tide]

Figure 23. [Close up of the water level derived contour lines]

#### 4.2.4 Photogrammetry

The first attempt to create a photogrammetric model included using GPS GCP's 1 - 7, as well as two extra GPS GCP's that were not used for rectification. (Figure 24) contains all locations from where an image was captured, as well as the image overlap throughout the area. After alignment of photos, the GCP's were dragged to their appropriate positions in all images where they could be found. After the dragging of the GCP's a low quality 3D point cloud was generated. The 3D model had small errors in the x,y direction, however the z-direction showed errors of up to 40 meters, warranting further correction.

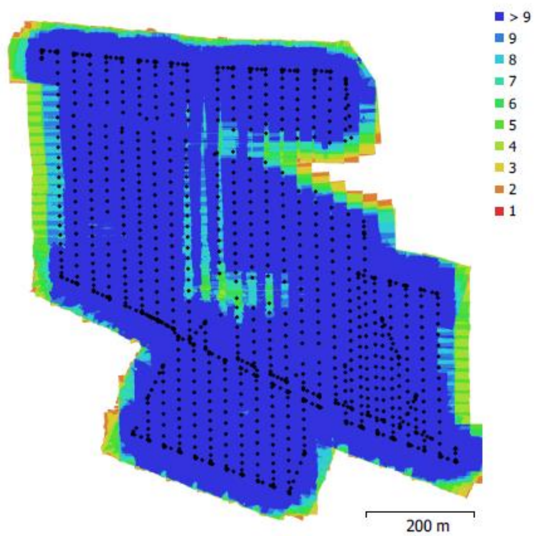


Figure 24. [Black dots show locations of image capture, colours mark the number of overlapping pictures throughout the area]

The only possible intervention to be made was the addition of more GCP's. Google Maps based GCP's were not feasible, due to their inaccuracy compared to the GPS GCP's, especially in terms of z-values. It was not possible to go back into the field to measure more points. Instead new GCP's were created with the aid of the raw imagery used for rectification. Four landmarks on the riverbanks were selected that were easily recognizable in the photogrammetry images and at the same time were found to be intersecting with the water line in one of the raw images used for rectification. The x,y values of those points were obtained from the x,y,z values found in the aforementioned low quality 3D point cloud. The z-values were taken from the water level data, as the landmarks were found to be intersecting with the waterline.

With the addition of the four new GCP's, the photogrammetric process was reverted back to the step after photo alignment. The four new GCP's were added to the set of existing GCP's, now containing 13 GCP's, shown in (Figure 25) and (Table 4). After dragging the GCP's to their appropriate position a new low quality 3D point cloud was generated, the total RMS values of the GCP's are shown in (Table 5). After manually erasing outliers from the point cloud, the high quality point cloud, Orthophoto (Figure 26) and DEM (Figure 27) were generated. No editing of the DEM was done after generation. The current DEM illustrates the poor water handling of the software, having values of -120 meters, narrowing the range of the scale bar will enhance it's potential to study features on the riverbank. The addition of the new GCP's caused the z-error to be reduced from ~40meters to 0.18 meters. Both the X and Y error are high, considering the millimeter accuracy of the GCP's. Individual inspection of GCP errors showed that most GCP's had errors in the millimeter range, whereas the GCP's with errors of several meters were all located in the top right corner of the covered area.

| GCP's | Run 1 | Run 2 |
|---|---|---|
| GPS 1 | x | x |
| GPS 2 | x | x |
| GPS 3 | x | x |

| | | |
|---|---|---|
| GPS 4 | x | x |
| GPS 5 | x | x |
| GPS 6 | x | x |
| GPS 7 | x | x |
| GPS 8 | | |
| New GCP 1 | | x |
| New GCP 2 | | x |
| New GCP 3 | | x |
| New GCP 4 | | x |

Table 4. Overview of GCP's used in the first and second photogrammetry run.

| Count | X error (m) | Y error (m) | Z error (m) | XY error (m) | Total (m) |
|---|---|---|---|---|---|
| 13 | 1.44423 | 0.430428 | 0.18293 | 1.50701 | 1.51807 |

Table 5. [The RMS error for all 13 GCP's]

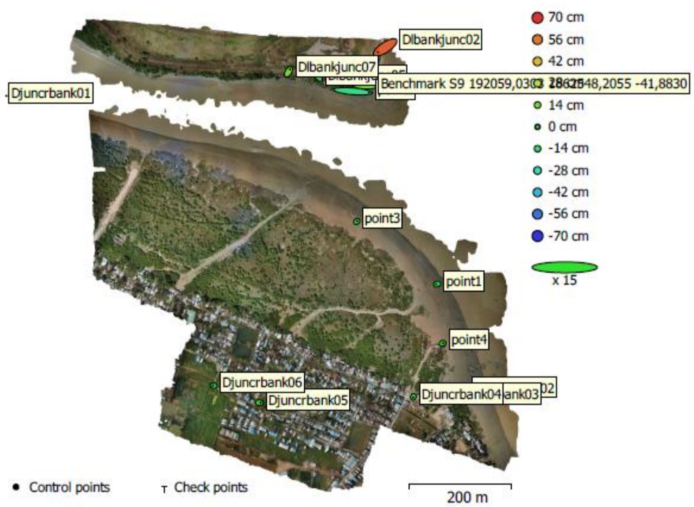


Figure 25. [GCP's projected on Orthophoto of the research area]

Figure 26. [Orthophoto of the Pan Hlaing – Yangon river research area]

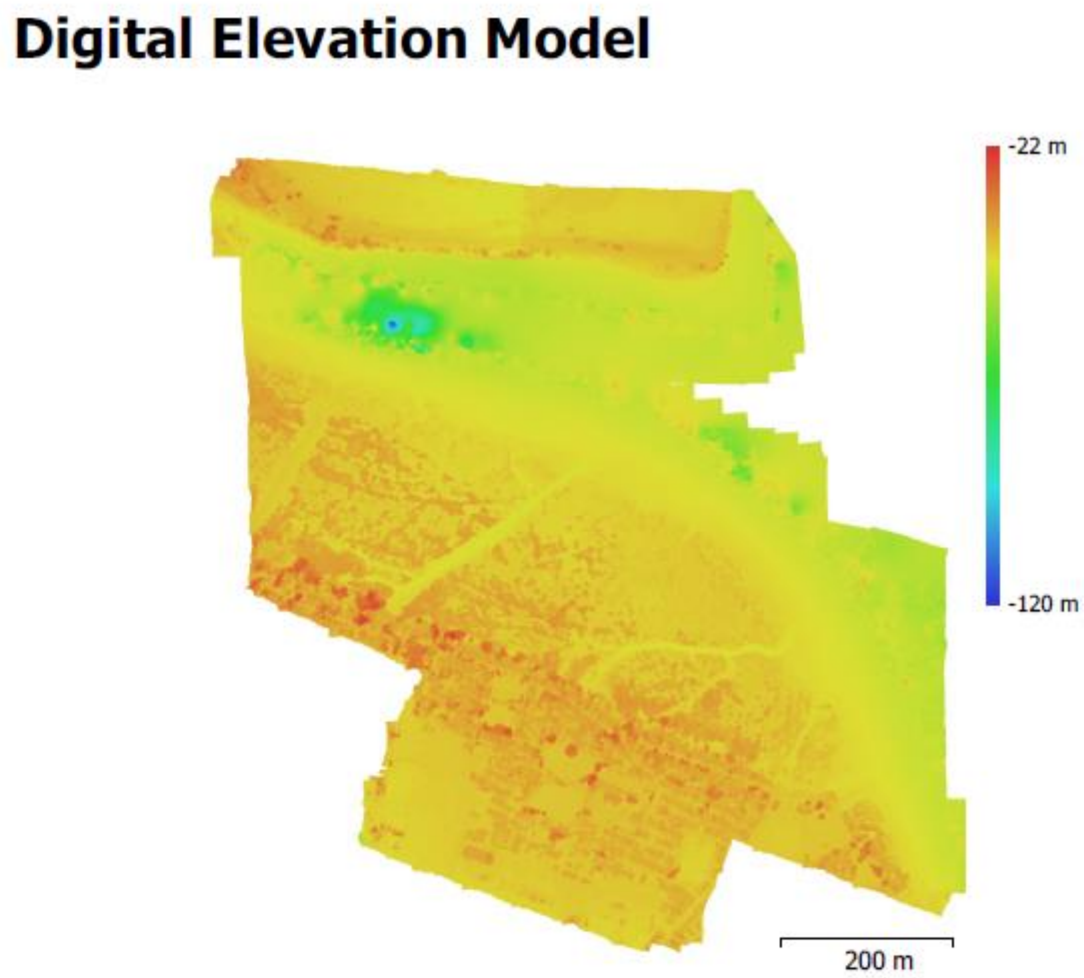


Figure 27. [DEM of the research area, colors represent elevation. Blue colors are anomalies by poor water handling of the software.]

## 5. Discussion

The research completed a full drone survey, from fieldwork to finalized products in the form of rectified imagery including contour lines of the intertidal zone and a photogrammetry based DEM and Orthophoto. As can be seen in the results, the process was not without complication. In this section the various components of the methodology will be discussed, which will lead up to the answering of the research questions in the conclusion.

### 5.1 Ground Control Points

Within the research there has been plenty experimentation with all types of GCP's, including the use of satellite imagery for creating GCP's. First the use of manually placed GCP's will be discussed, after that the use of natural or man-made objects and finally the use of satellite imagery to create GCP's.

### 5.1.1 Manually placed GCP's

Manually placed GCP's have only been used at the Cofferdam and Mezali Sluice. This proved necessary as there were insufficient natural or man-made objects to be used. The first difficulty encountered was the innate risk of theft and movement of manual placed GCP's. Although both areas were sparsely populated, theft occurred at both locations. At Mezali Sluice an obvious cause would be the large amount of children, to which a brightly colored GCP can be attractive. At the Cofferdam it was more likely to be a deliberate attempt to frustrate the work given the absence of children and a hostile encounter with local residents during flight (see section 4.1.3).

Possible theft mitigation can be the placement of extra GCP's, to offset a possible loss. Another option would be to try and inform residents of the research done. Although not encountered, more risky is the movement of a GCP, if a moved GCP is included in the processing it could jeopardize the accuracy of the entire project. Movement can be visually indicated during picking up GCP's after research, to be safe one could consider to re-measure each GCP upon pickup.

Another point of attention is visibility of the GCP to be used. When the distance from camera to object increases, by higher flight altitude or an oblique camera angle, the visibility of a GCP decreases. First the target (See Figure 10) on the GCP could become indistinguishable, reducing the possible accuracy, ultimately the GCP might not be recognized in the image all together. Sufficiently sized GCP's of which the color is in contrast with the surroundings, are thus paramount to a successful survey.

### 5.1.2 Fixed objects and landmarks

Fixed objects and landmarks were the only type of GPS measured GCP's used in the focus area of this research. The most difficult part was finding enough objects or landmarks to gain a desired GCP coverage and density. For rectification, preferably GCP's are selected flat on the ground, as the location of an elevated GCP in an oblique image is distorted due to perspective. In terms of visibility the same rules as with manual placed GCP's apply, the object chosen should be of sufficient size and one could consider highlighting it with paint to increase visibility.

The added benefit is that the GCP's are relatively immovable, with no risk of theft. This becomes increasingly beneficial when setting up a monitoring project. After measurement the GCP's can be reused when performing multiple surveys over time. The effort involved with manual placed GCP's will multiply when having to reinstall them time and time again. One could consider leaving them in place, but this will greatly increase the risk of GCP movement and removal.

### 5.1.3 Use of satellite GCP's

Satellite derived GCP's, which are natural or man-made objects, have been of great aid in this research. GPS measured GCP's covered only the bottom $1/3^{rd}$ of the images to be rectified. Two out of 6 satellite based GCP's greatly aided in improving the rectification accuracy, whilst the other four being used as checkpoints, allowing for judgment of the quality of rectification in areas that would otherwise have no GCP coverage.

The downside of using satellite imagery, is that the quality of geo-referencing ads further inaccuracy which in this case was approximated to be 3.72m on average, yet varying from point to point. Having accurately measured points in the area is essential to estimate geo-referencing of the satellite map. Without any source of comparison, the unknown geo-referencing leaves a gap in the accuracy analysis of the final product.

Satellite derived GCP's were also considered for photogrammetric use. Unfortunately the satellite map elevation data has a resolution of 1-arc second or 30m, meaning the elevation is averaged for tiles of approximately 30 by 30 meters, which is useless for most photogrammetry projects.

Another point of attention is the resolution, which determines the accuracy of which the location of a GCP can be selected. However this factor is minor compared to the accuracy of geo-referencing. Given the accuracy constraints, the usability of satellite derived GCP's depends on the accuracy aim. The accuracy constraints will have more impact on projects undertaken with low flight altitudes and camera angles, whereby to distance from camera to GCP is lower and a higher accuracy would have been possible. One could consider using paid satellite maps, which usually have a higher resolution, but geo-referencing is still an issue for these maps (Aguilar et al., 2017).

## 5.2 Flying and capturing imagery

Flying and capturing imagery has been relatively uncomplicated. The limitations in terms of equipment have been the battery life of both the Drone's batteries and the batteries the devices (smartphone or tablet) running the flying software. When wanting to survey a full day, logistics of charging are going to be a bottleneck, therefore it is advisable to bring or find a power source in the field.

The use of manufacturer and third party software, such as DJI-GO and Pix4Dcapture greatly assisted in the ease of flying. Usage of such software however also poses some constraints. For a most consistent series of rectified image, ideally the images are shot at the same location with the same camera orientation. Using DJI-GO it was possible to set waypoints, however hovering at a waypoint still had to be initiated manually, leading to slightly different hovering positions. Also the camera still had to be controlled manually, leading to slightly different angles of image capture. Pix4D had restrictions on the distance the drone was allowed to fly away from the user. The preference was to use long distance rectangular flight patterns to minimize the amount the drone had to turn to another flight line, hereby saving precious battery power, but due to the restriction less elongated plans involving more turns had to be used.

The amount of software being further developed or newly released to aid with flying is rapidly increasing, probably offering more freedom of operation in the future. For an ultimate customized experience there is the possibility of developing your own software. This could even be coupled with building your own drone (Sa et al., 2018), for which guidelines are readily available. Building one's own software and drone will however require significant technical knowledge and an investment of time. Yet the freedom gained might be interesting for professional use.

## 5.3 Rectification and Photogrammetry Error Analysis

This section attempts to identify the sources having the greatest impact on the RMS error, starting with analysis of the 4 steps of rectification and afterwards analyzing photogrammetry. Accurate pinpointing of error sources will be difficult, because the various components contributing to the error are dependent upon each other. In the third step of rectification, it was found that the previously used camera parameters greatly contributed to the overall error, this may also have an effect on the choices made in step 1 and 2. Due to time constraints it was not possible to revisit step 1 and 2, therefore the error sources of step 1 and 2 are analyzed whilst keeping the effect of the camera parameters in mind.

When analyzing the RMS expressed in meters, it should also be taken in account that the pixel sizes of a rectified image are not equal. Due to the increasing pixel-size when moving away from the camera, a pixel shift in the back of the image is going to have a greater contribution to the RMS in meters as compared to a pixel in the front of the image, even if the shift in pixels is similar. Analyzing the RMS in pixel units would thus give a more absolute measure of accuracy. Unfortunately the analysis of pixel RMS was only introduced in the last rectification step, again due to time constraints it was not possible to revisit previous steps. In the end the RMS in meters is going to be more suitable for determining the applicability of rectification in scientific and commercial projects, as accuracy standards are generally not expressed in pixels.

*Analysis of step 1:*

The first step of the rectification process led to discarding of GCP 2, 7 and 8. The exclusion of these GCP’s contradict the finding of (Martínez-Carricondo et al., 2018), according to which a higher amount and density of GCP’s will lead to more accurate results. Exclusion of GCP 2 can be due the fact it’s located on an elevated structure, causing a slight shift in location due perspective distortion. The camera distortion can also play a role, which is strongest at the edges of the image (see Figure 11 & 12) where GCP 2 is located. For GCP 7 there is no obvious reason. Possibly the high density of GCP’s near GCP 7 biases the rectification towards that location, thereby worsening rectification in other locations.

Within the first step the top 2/3$^{rd}$ of the image is poorly rectified, one would expect that using GCP 8 could aid in correcting the upper part of the image, however the opposite was the case. GCP 8 is located towards the top edge of the image, therefore possibly suffering from strong camera distortion. Another contribution can be found in the manual selection process of the pixel coordinates. The image gets coarser towards the top, due which the exact location of GCP 8 cannot be recognized and only approximated. This easily leads to GCP selection being a few pixels off, and as the pixel sizes are at its largest in the upper portion of the image, the resulting error contribution in meters is also increased.

*Analysis of step 2:*

Increasing GCP amount and density by the addition of all 6 GCP’s did not lead to a lower total RMS. An obvious contributor would be the average 3.72m error of the Google Maps GCP’s themselves. However the magnitude of change in total RMS in between the various runs, including a subset of the 6 new GCP’s, were far greater than their inherent inaccuracy. Furthermore addition of Google Maps GCP 2 and 4 did lead to a significant lowering of the total RMS by nearly 20m. Therefore there is likely another mechanism into play.

Just like GCP 8, the Google Maps GCP’s are further towards the top of the image as compared to the other GPS GCP’s. The error by these GCP’s could thus follow the same mechanism, with a greater chance of being a few pixels off in manual GCP selection and the error in meters being magnified due to the increase of pixel size. This is not likely to be the main mechanism, as inclusion GCP 2 and 4 did decrease the RMS error. Individual inspection shows that inclusion or exclusion of GCP 3 has the least effect on the error, with GCP 1, 5 and 6 having the greatest effect. GCP 1, 5 and 6 are all located near the edge of the images, where the effect of distortion is going to be greatest (See Figure 11 & 12), therefore the main influence is likely the camera parameters.

*Analysis of step 3:*

The results of the third step highlight the importance of a proper camera calibration. The main contributors to heightening of the total RMS seems to be the distortion parameters, however the internal camera parameters also have a contribution. For the internal camera parameters, using the matrix estimated by Agisoft photoscan yielded better results. Using the distortion from Agisoft caused significant lowering of the total RMS, however results further improved when disregarding the distortion at all. Since disregarding the distortion caused the lowest RMS, it can be concluded that both the original and Agisoft based camera parameters overestimate the distortion. Section 5.4 will have a more in depth look at the method used for obtaining the camera parameters, whilst offering solutions for a better estimation of the camera parameters.

*Analysis step 4:*

When looking at the RMS values for all 5 images, it can be seen that the pixel RMS and meter RMS vary shows between the images. The effect of exclusion of GCP(s) in image 4 and 5 is not known and will be assumed to have no significant effect. Other than the pictures having a slightly different camera angle, there is no external factor which can explain the variations of RMS in replication. The only inconsistent factor in replication is the process in which the pixel coordinates of the GCP's are manually selected.

*Photogrammetry Accuracy*

Compared to rectification accuracy which shows GCP errors of several meters, the accuracy of the photogrammetry work is much higher, with an average XY error of 1.5 meters. Still the accuracy has the potential to be in the millimeter range, just like the accuracy of the GCP's used. Manual selection of the GCP locations is not likely to be the culprit, due to the 50m height of image capture and the camera having a 90$^o$ angle to the ground, all GCP locations were easily recognizable. Inspection of the individual GCP's showed that the error originates from the GCP's clustered in the top right corner of the model. No certain reason for this error was found, however most likely it originates from the processing phase. Between the creation of a low and high quality point cloud, outlying points often originating from poor handling of vegetation, should be erased. If some outliers were missed, their inclusion in the high quality point cloud could cause an increased error at the locality of these outliers. The z-error is around 0.18m, yet also has the potential to be in the millimeter range. Individual inspection shows that the GCP's with the highest error are the same GCP's responsible for the majority of the XY error, therefore the same mechanism is thought to be responsible.

## 5.4 Camera Calibration

As became apparent during the rectification process the camera matrix obtained during calibration had a severe negative impact on the accuracy of the final results. This could be due to errors in the calibration procedure, or due to external circumstances inherent to the research. Some of the errors that could have occurred during the calibration are:

- Geometric errors made by the printer.
- Environmental conditions such as changing temperature and moisture causing the checkerboard paper, or the wood to which the paper was taped, to deform.
- Blurry images obscuring the checkerboard crossings due to poor light conditions or incorrect focusing of the camera.

Out of these only blurry images could be readily checked and some of the images used in the calibration procedure were indeed blurry. Errors such as indicated above could be avoided by:

- Using an industrial grade printer.
- Printing the checkerboard image directly on a solid material with low sensitivity to thermal and moisture deformation.
- Performing the calibration in controlled environmental conditions, such as found in a laboratory.
- Familiarizing yourself with the camera and correct focusing before taking images used for calibration.

Doing so will increase the cost and effort of calibration, yet should be considered as the calibration is one of the fundamentals governing accuracy. The reprojection error of the calibration gives a measure of the accuracy quality of the calibration. Although there are no strict rules to judge the quality of calibration by the reprojection error, an error closer to zero means a better calibration, with the author of the calibration script ("GoPro Lens Calibration and Distortion Removal", 2018) stating that a reprojection error below 0.1 indicates a good calibration. The reprojection error found in this research was 0.046456 pixels, which is well below 0.1. Therefore it is unlikely that the quality of the calibration is the main driver behind the large errors found in rectification, which suggests that other mechanism are at play.

Changes in temperature during image capture also affects the internal geometry of the camera (Smith & Cope, 2010). This likely played a role, since calibration was performed under room temperature (20 $^{o}$C), whilst temperatures encountered in the field reached up to 40 $^{o}$C. This issue is hard to solve, given that weather conditions are subject to change. It is best mitigated by calibrating the camera under conditions that are most likely encountered in the field.

Yet another factor not taken in account in this research is that of the focus distance. A change in focus distance causes physical changes in the lens configuration, resulting in a change of principal distance and lens distortion (Sanz-Ablanedo et al., 2012). The calibration was undertaken at close range, whilst the imagery used was taken at long range. Certainly distortion parameters obtained do not suit the circumstances of image capture. To overcome this issue, (Sanz-Ablanedo et al, 2012) have proposed a method of parameterizing the internal camera and distortion parameters according to focusing distance. A more crude method would be to fix the camera focus at hyper focal distance, which is the closest focus distance after which any point on the background will become sharp. Based on user reviews, the hyper focal distance of the Mavic Pro is around 10meters, which is still a realistic distance for undertaking calibration. The challenge will be to fix the focus distance at hyper focal distance. In old mechanic cameras this is straightforward, but for present day digital cameras tinkering with the camera firmware might be necessary.

## 5.5 Law, Regulations and Ethical Considerations

Understanding of local law and regulation, as well as taking in account ethical issues such as privacy can be vital for the success of any drone-based survey. As often encountered with rapidly emerging technology, the corresponding legal framework lags behind (Stöcker et al., 2017). This was evident in this research, the government officials of the Irrigation Department did not refer to concrete laws or regulation, yet suggested a letter of permission before any work took place. Their concern for flying at the Pan Hlaing – Yangon river junction was most likely due to the area being an economic hotspot with nearby sensitive facilities such as a military base and oil terminal.  The decision does fit in with the international trend of risk-based regulation, taking in account factors such as flight area, purpose and visibility. (Stöcker et al, 2017) For future research it is thus suggested to take in account the national laws and regulations and how they apply to the local environment of the research area. When needed, a request of flight permission should be made well in advance, which will avoid unnecessary downtime.

After obtaining flight permission, further difficulty was encountered regarding privacy issues of local citizens. The disruption of work was minor, but similar more difficult situations could become a reality for drone users. Literature study by (Luppicini & So, 2016) highlights widespread safety, privacy and ethical concerns, referring to the lack of laws and regulations to relieve those concerns. Lacking a legal framework, identifying and addressing these concerns are mainly the responsibility of the drone user. One could consider informing local citizens before taking to the sky, or at least be prepared to explain the nature of your work. Other than addressing ethical considerations, preventive measures will also minimize the chance of work disruption.

## 5.6 Important findings and recommendations

The most important findings and recommendations will be summarized following the order of the discussion.

- Satellite based GCP’s can greatly reduce the effort of measuring GCP’s in the field. The downside is the added inaccuracy due to the quality of geo-referencing of the satellite maps and the need for a method to quantify this inaccuracy. Lack of high resolution elevation data makes satellite GCP’s only usable for rectification.

- Flying and capturing imagery is mostly limited by battery life and software used for flying. This is however likely to improve with the rapid development of the drone industry. With proper skill and effort customization of equipment and software is possible.

- Manual selection of GCP location in the rectification processing phase causes inaccuracy and limits reproducibility. The potential and impact of error increases further away from the camera, where the image gets coarser and pixel size increases.

- Within this research the camera calibration was the main contributor to inaccuracy of rectification. Calibration quality can be increased by changes in the calibration procedure, however more gain could be had by accounting for the physical changes in the lens configuration due to changing focus distance.

- Laws and regulation lag behind the technological development of drone usage and can be expected to change in the future. Failure to take in account law and regulation applicable to the country and area of fieldwork could cause significant delay or obstruction of work.

- Ethical issues in terms of privacy concerns of inhabitants in the research area can be encountered. Be prepared to, perhaps preemptively, explain the nature of the work done to avoid obstruction and delay.

Within the conclusion the research question and sub-questions will be answered, together with a look into the possible roles drones could fulfill in coastal and delta surveying.

## 5. Conclusion

To conclude each of the sub-questions and the main-research question will be answered.

1. *Can fixed objects with coordinates derived from satellite maps serve as an alternative to manually placed ground control points?*

Theft and movement of manually placed GCP's was found to be a problem in this research. Usage of man-made or natural occurring objects did provide a solution to this problem, at the cost of freedom of placement in any desired location. When the GCP's are still measured in the field, the reduction in effort only becomes apparent in a monitoring project where GCP's are used for multiple surveys. Effort can be significantly reduced when obtaining the GCP's coordinates with satellite maps. The downside is the error in geo-referencing found in the satellite maps, which directly affect the accuracy of the GCP's. If the quality of geo-referencing is unknown, it is still necessary to go into the field with GPS equipment to obtain points used for quantifying the geo-referencing error, negatively impacting the reduction of effort. Satellite based GCP's are unfortunately not usable for photogrammetry, due to the maps having low resolution elevation data.

2. *Which are the main factors influencing the accuracy of the final products?*

The accuracy is influenced by multiple factors, both while gathering and processing the data. During the gathering of data the accuracy is influenced by the amount and density of GCP's measured, as well as the accuracy of measurement of the GCP's. The accuracy is further influenced by the height of flight and for rectification the angle of image capture, increasing the pixel sizes and determining the visibility of GCP's in the imagery. During data processing the manual selection of GCP's adds a source of error, directly influenced by the aforementioned pixel sizes and visibility of GCP's. Quality of camera calibration was a major source of accuracy loss in this study, some of which can possibly be prevented by a more precise calibration procedure. Best results were had when ignoring the lens distortion parameters. Usable distortion parameters can likely be obtained by taking in account the change of distortion due to changes in camera focal distance.

3. *Which factors, not covered in the previous questions, should be taken in account for conducting a successful drone survey?*

One important factor is the equipment and software used for conducting the survey. Gathering imagery is mainly limited by battery life of the drone, whilst the software used can pose limitations on freedom of flight mission planning. As drones and accompanying software are rapidly developing, the choice of equipment and software will increase in the future.

Laws and regulation should not be ignored, doing so could cause delay in work. Law and regulation will vary between countries and their applicability is likely dependent on the environment of the research area. Laws and regulation are still under development and will impact the ease of professional drone use in the future.

Drones could cause privacy concerns for inhabitants of the research area. Explanation of the kind of work that is being conducted should not only be considered from an ethical viewpoint but could also prevent unwarranted obstruction of work.

The final and main research question to be answered is: *To what extent can consumer drones be used for surveying of deltaic and coastal systems?*

Drones are especially useful in deltaic and coastal settings due to ability to cover hard to access terrain. The availability of easy to use dedicated software makes drone-based photogrammetry an accessible tool to gather topographic data for any drone owner. Rectification shines in its potential for mapping a large area using only a single image. As demonstrated in this research, rectification of multiple images offers an opportunity to study more dynamic environments such as the intertidal zone. Combination with other tools such as water level loggers broadens the possibility of rectification, by adding a 3D component. The usefulness of both techniques is partly determined by the obtainable and desired accuracy of any project. Further development of the rectification technique should aim at heightening its accuracy, which is most likely achieved by addressing the issues regarding camera calibration. The drone industry is rapidly developing, causing drones with higher technical capabilities at a lower cost to enter the market. Combined with their ease of use, drones could become major players in the field of surveying for both commercial, governmental and scientific parties.

# 6. References


Aarnink, J. (2017). Bathymetry Mapping using Drone Imagery (Postgraduate). Delft University of Technology. uuid:d607109b-5891-46bc-8670-fc9b99a2b409

Aguilar, M., Nemmaoui, A., Aguilar, F., Novelli, A., & García Lorca, A. (2017). Improving georeferencing accuracy of Very High Resolution satellite imagery using freely available ancillary data at global coverage. *International Journal Of Digital Earth*, *10*(10), 1055-1069. doi: 10.1080/17538947.2017.1280549

ARGUS video systems - Deltares. (2018). Retrieved from https://www.deltares.nl/en/projects/argus-video-systems

Bhardwaj, A., Sam, L., Akanksha, Martín-Torres, F., & Kumar, R. (2016). UAVs as remote sensing platform in glaciology: Present applications and future prospects. Remote Sensing Of Environment, 175, 196-204. doi: 10.1016/j.rse.2015.12.029

Chikhradze, N., Henriques, R., Elashvili, M., Kirkitadze, G., Janelidze, Z., Bolashvili, N., & Lominadze, G. (2015). Close Range Photogrammetry in the Survey of the Coastal Area Geoecological Conditions (on the Example of Portugal). Earth Sciences, 4(5), 35. doi: 10.11648/j.earth.s.2015040501.17

Diver Manual. (2014). [ebook] Delft: Schlumberger Water Services. Available at: https://www.swstechnology.com/novametrix/pdfs/equipment/Diver_manuals/Diver_Product_Manual_en.pdf [Accessed 15 Dec. 2018].

DJI Official. (2018). DJI GO - Capture and Share Beautiful Content Using this New App. [online] Available at: https://www.dji.com/goapp [Accessed 15 Dec. 2018].

Docs.opencv.org. (2018). Camera Calibration and 3D Reconstruction — OpenCV 2.4.13.7 documentation. [online] Available at: https://docs.opencv.org/2.4/modules/calib3d/doc/camera_calibration_and_3d_reconstruction.html [Accessed 15 Dec. 2018].

GoPro Lens Calibration and Distortion Removal. (2019). Retrieved from https://www.theeminentcodfish.com/gopro-calibration/

Guillot, B., Castelle, B., Marieu, V., Bujan, S., & Rosebery, D. (2018). UAV monitoring of 3-year Foredune Partial Recovery from a Severe Winter: Truc Vert Beach, SW France. Journal Of Coastal Research, 85, 276-280. doi: 10.2112/si85-056.1

Hage, P., Ruessink, B. and Donker, J. (2018). Determining sand strip characteristics using Argus video monitoring. Aeolian Research, 33, pp.1-11.

Hemmelder, S., Marra, W., Markies, H., & De Jong, S. (2018). Monitoring river morphology & bank erosion using UAV imagery – A case study of the river Buëch, Hautes-Alpes, France. International Journal Of Applied Earth Observation And Geoinformation, 73, 428-437. doi: 10.1016/j.jag.2018.07.016

Hoonhout, B. (2014). Source code for flamingo.rectification.rectification. Retrieved from http://www.openearth.nl/flamingo/_modules/flamingo/rectification/rectification.html

Immerzeel, W., Kraaijenbrink, P., Shea, J., Shrestha, A., Pellicciotti, F., Bierkens, M., & de Jong, S. (2014). High-resolution monitoring of Himalayan glacier dynamics using unmanned aerial vehicles. Remote Sensing Of Environment, 150, 93-103. doi: 10.1016/j.rse.2014.04.025

Luppicini, R., & So, A. (2016). A technoethical review of commercial drone use in the context of governance, ethics, and privacy. Technology In Society, 46, 109-119. doi: 10.1016/j.techsoc.2016.03.003

Martínez-Carricondo, P., Agüera-Vega, F., Carvajal-Ramírez, F., Mesas-Carrascosa, F., García-Ferrer, A. and Pérez-Porras, F. (2018). Assessment of UAV-photogrammetric mapping accuracy based on variation of ground control points. International Journal of Applied Earth Observation and Geoinformation, 72, pp.1-10.

Mavic Pro User Manual V2.0. (2017). [ebook] DJI. Available at: https://dl.djicdn.com/downloads/mavic/20171219/Mavic%20Pro%20User%20Manual%20V2.0.pdf [Accessed 15 Dec. 2018].

Neumann, B., Vafeidis, A., Zimmermann, J., & Nicholls, R. (2015). Future Coastal Population Growth and Exposure to Sea-Level Rise and Coastal Flooding - A Global Assessment. *PLOS ONE*, *10*(3), e0118571. http://dx.doi.org/10.1371/journal.pone.0118571

Opencv.org. (2018). OpenCV library. [online] Available at: https://opencv.org/ [Accessed 15 Dec. 2018].

Sa, I., Kamel, M., Burri, M., Bloesch, M., Khanna, R., & Popovic, M. et al. (2018). Build Your Own Visual-Inertial Drone: A Cost-Effective and Open-Source Autonomous Drone. *IEEE Robotics & Automation Magazine*, *25*(1), 89-103. doi: 10.1109/mra.2017.2771326

Sanz-Ablanedo, E., Chandler, J., & Wackrow, R. (2012). Parameterising Internal Camera Geometry with Focusing Distance. The Photogrammetric Record, 27(138), 210-226. doi: 10.1111/j.1477-9730.2012.00677.x

Schenk, T. (2005). Introduction to Photogrammetry. [ebook] Columbus: Department of Civil and Environmental Engineering and Geodetic Science, The Ohio State University. Available at: https://pdfs.semanticscholar.org/7ed2/25c0799608539512fd84597892a5eb03e0b3.pdf [Accessed 5 Nov. 2018].

Smith, M., & Cope, E. (2010). THE EFFECTS OF TEMPERATURE VARIATION ON SINGLE-LENS-REFLEX DIGITAL CAMERA CALIBRATION PARAMETERS. International Archives Of Photogrammetry, Remote Sensing And Spatial Information Sciences, Vol. XXXVIII, Part 5.

Stöcker, C., Bennett, R., Nex, F., Gerke, M., & Zevenbergen, J. (2017). Review of the Current State of UAV Regulations. *Remote Sensing*, 9(5), 459. doi: 10.3390/rs9050459

Webb, E., Friess, D., Krauss, K., Cahoon, D., Guntenspergen, G., & Phelps, J. (2013). A global standard for monitoring coastal wetland vulnerability to accelerated sea-level rise. Nature Climate Change, 3(5), 458-465. doi: 10.1038/nclimate1756

Wu, S. (1985). Digital image transformation and rectification of spacecraft and radar images. Photogrammetria, 40(2), 119-134. doi: 10.1016/0031-8663(85)90006-7

Zhang, J., Hu, J., Lian, J., Fan, Z., Ouyang, X., & Ye, W. (2016). Seeing the forest from drones: Testing the potential of lightweight drones as a tool for long-term forest monitoring. *Biological Conservation*, 198, 60-69. doi: 10.1016/j.biocon.2016.03.027